

## Hard-mode infrared study of the ferroelastic phase transition in $\text{CuWO}_4\text{-ZnWO}_4$ mixed crystals

Simon A. T. Redfern

*Department of Geology and Department of Chemistry, University of Manchester, Manchester M13 9PL, United Kingdom*

(Received 25 February 1993)

The  $P\bar{1}$ - $P2/c$  ferroelastic phase transition in  $\text{Zn}_{0.75}\text{Cu}_{0.25}\text{WO}_4$  has been studied as a function of temperature by infrared spectroscopy. Many of the midinfrared features (associated with  $\text{WO}_6$  octahedral vibrations) do not show coupling to the transition. However, the Jahn-Teller distortion of the  $\text{CuO}_6$  octahedra induces a large change in the frequency of the  $1190\text{-cm}^{-1}$  phonon near  $T_c$  ( $=570\pm 5\text{ K}$ ). Concomitant broadening of this absorption band in the vicinity of  $T_c$  arises either from a dynamic isospin-flip mode at the Cu site, or solitonic excitations associated with the ferroelastic microstructure. The high-temperature phase does not appear to consist of disordered  $P\bar{1}$  domains; rather, the transition appears essentially displacive in character.

### I. INTRODUCTION

Transition-metal tungstates are a technologically important group of materials,  $\text{ZnWO}_4$  and  $\text{CuWO}_4$  having particular prominence in their potential application as materials for scintillation detectors, laser hosts, photoanodes, and optic fibers. As a result, there has been much interest in both  $\text{ZnWO}_4$  and  $\text{CuWO}_4$ , and a significant body of work exists devoted to the understanding of their physicochemical properties. Only recently, however, has attention turned to the properties of mixed crystals of composition  $(\text{Zn}_x\text{Cu}_{1-x})\text{WO}_4$ , which form a solid solution between the end members.<sup>1</sup>

The  $(\text{Zn}_x\text{Cu}_{1-x})\text{WO}_4$  solid solution displays a ferroelastic structural phase transition, between the triclinic  $P\bar{1}(C_i)$   $\text{CuWO}_4$  structure and the monoclinic  $P2/c(C_{2h})$   $\text{ZnWO}_4$  structure, on increasing  $\text{ZnWO}_4$  content at a composition  $\text{Zn}_{0.78}\text{Cu}_{0.22}\text{WO}_4$ .<sup>1</sup> The transition temperature increases rapidly from room temperature with increasing  $\text{CuWO}_4$  content (Fig. 1). The transition is associated with critical phonons at the center of the Brillouin zone; the order parameter for the transition transforms as

the active representation  $B_g$ , in the  $P2/c$  supergroup. The time-averaged behavior of the long-range order parameter has been investigated in a series of x-ray scattering<sup>1,2</sup> and absorption<sup>3,4</sup> studies of the solid solution, and described within the framework of a classical Landau model. The driving mechanism for the transition has been related to the Jahn-Teller-induced distortion of the  $(\text{Zn,Cu})\text{O}_6$  octahedra with increasing Cu content. This effect induces a large triclinic distortion on these octahedra, most clearly seen by comparison of the structures of the two end members. In  $\text{ZnWO}_4$ , the point symmetry of both the W and Zn sites is  $C_2$  with three pairwise equivalent bonds in each octahedron, Zn-O bond lengths lying between 2.06 and 2.14 Å.<sup>5</sup> In  $\text{CuWO}_4$ , however, removal of the degeneracy of the  $3d$  orbitals results in the lengthening of two opposite Cu-O bonds to 2.4 Å in an elongated octahedron,  $\text{Cu}^{2+}$  being approximately square-planar coordinated by four oxygens at a distance of  $1.98\pm 0.02$  Å in a  $C_1$  site.<sup>6,7</sup> By contrast, the  $\text{WO}_6$  octahedra in  $\text{CuWO}_4$  are only slightly distorted, by off centering of the tungsten atom.

Whether the  $P\bar{1}$ - $P2/c$  transition is driven by a pure acoustic soft mode, by another displacive process, or has some degree of order-disorder character has not yet been addressed, since studies have concentrated on the description of the average long-range characteristics of the transition. There is no indication whether the  $P2/c$  high-temperature phase represents a disordered form of the  $P\bar{1}$  phase or a homogeneous ordered  $P2/c$  structure. Fluctuation-related line broadening of certain Bragg reflections in powder x-ray-diffraction patterns near  $T_c$  has been noted, however, and indicates that dynamical local fluctuations may play a significant part in the high-temperature behavior.<sup>2</sup>

The use of hard-mode infrared spectroscopy as a probe of local strain, order-disorder, and related critical phenomena at structural phase transitions is now well established.<sup>8-12</sup> Here, the results of a high-temperature hard-mode infrared study of  $\text{Zn}_{0.75}\text{Cu}_{0.25}\text{WO}_4$  are reported and the nature of the high-temperature  $2/c$  structure is discussed. High-temperature x-ray diffraction showed that material of this composition is triclinic at room tempera-

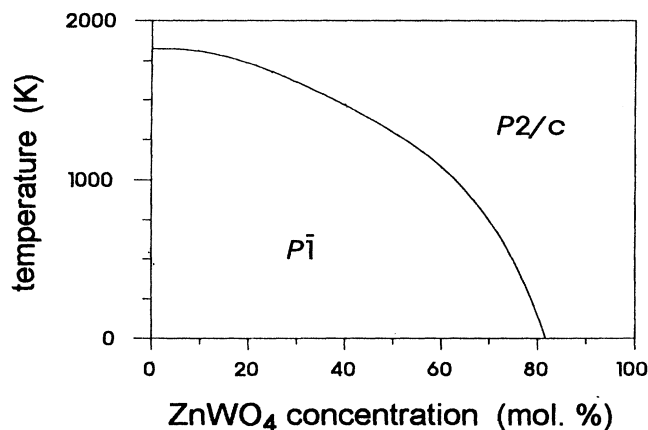


FIG. 1. Phase diagram of the  $\text{CuWO}_4\text{-ZnWO}_4$  system [ignoring melting, after (Ref. 2)].

ture and on increasing temperature transforms to the monoclinic polymorph at  $568 \pm 5$  K.<sup>2</sup> Coupling between the driving phonons for the transition and the infrared-active optic hard modes has been exploited to reveal the dynamic character of the transition, and further develop an understanding of the nature of the high-temperature phase.

## II. EXPERIMENTAL METHODS

The  $\text{Zn}_{0.75}\text{Cu}_{0.25}\text{WO}_4$  sample studied here was prepared by a direct precipitation method described elsewhere.<sup>1</sup> It is a member of the  $(\text{Zn}_x\text{Cu}_{1-x})\text{WO}_4$  solid solution and has been thoroughly characterized chemically using EPMA ATEM and  $2p$  soft x-ray-absorption spectroscopy, as well as structurally by x-ray diffraction and extended-x-ray-absorption fine structure.<sup>1-4</sup>

The dry crystalline sample was ground to a sub- $1\text{-}\mu\text{m}$  grain-size powder in the agate mortar of an electric ball mill, and thoroughly mixed with dry KBr dilutant in a ratio of 1:300, sample:KBr. A 200-mg, 13-mm diameter optically transparent disc was prepared by pressing the mixture at 75 MPa. A pure KBr disc was prepared in a similar manner and used as a reference for infrared measurements.

Absorption spectra were recorded under vacuum using a Bruker 113v Fourier transform infrared (FTIR) instrument. Spectra were measured between 400 and 2000  $\text{cm}^{-1}$  at a resolution of 2  $\text{cm}^{-1}$  using a liquid-nitrogen-cooled mercury cadmium telluride detector and KBr beam splitter. Increasing the scanning resolution did not reduce the widths of peaks measured at the temperatures of this study. The sample pellet was positioned within a cylindrical platinum-wound resistance furnace and held at temperatures between 300 and 733 K, measured using a Pt-Rh thermocouple held in contact with the sample pellet. Each spectrum was computed by Fourier transform of 250 interferometer scans using the controlling Aspect 3000 computer, and subsequently analyzed by least-squares fitting by Voigt profiles to determine the positions, intensities, and widths of absorption bands. Errors in measurements carried out by this method are estimated as  $\pm 0.5$   $\text{cm}^{-1}$  for peak positions and widths, and 10% for integrated intensities.

## III. RESULTS AND DISCUSSION

Spectra recorded between 300 and 733 K are shown in Fig. 2. Phonon resonances found are 546, 612, 622, 724, 804, 883, 1112, and 1191  $\text{cm}^{-1}$  at room temperature. The phonon spectra of intermediate Cu-Zn tungstates have not been recorded previously, and interpretation of the infrared spectrum depends heavily on a few results reported for the end-member materials  $\text{CuWO}_4$  and  $\text{ZnWO}_4$ .

Recent infrared studies on both  $\text{ZnWO}_4$  (Refs. 13-18) and  $\text{CuWO}_4$  (Refs. 19 and 20) report results only for frequencies greater than 2000  $\text{cm}^{-1}$ . An early reconnaissance, however, reported absorption at 880, 830, and 710  $\text{cm}^{-1}$  for  $\text{ZnWO}_4$  and 910, 800, and 740  $\text{cm}^{-1}$  for  $\text{CuWO}_4$ .<sup>21</sup> It will be noticed that the bands measured in

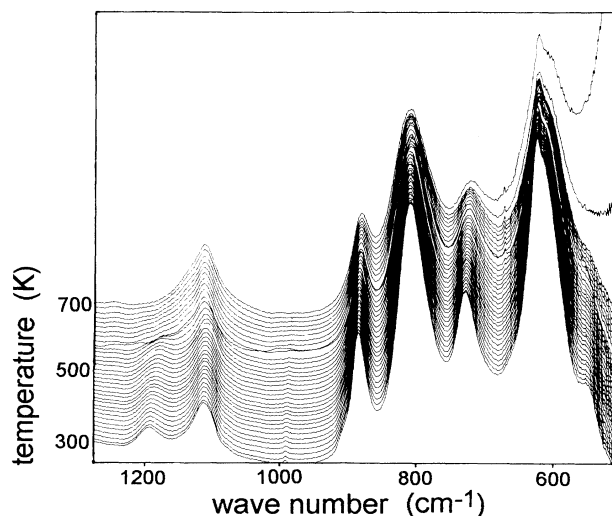


FIG. 2. Midinfrared powder absorption spectra of  $\text{Zn}_{0.75}\text{Cu}_{0.25}\text{WO}_4$  as a function of temperature. The rising background at low wave numbers in the highest-temperature spectra is a result of the high-temperature recrystallization of the KBr matrix of the pressed pellets.

$\text{Zn}_{0.75}\text{Cu}_{0.25}\text{WO}_4$  at 883, 804, and 724  $\text{cm}^{-1}$  fall partway between the values for the end-member phases, as would be expected for this member of the solid solution. Phonons in this frequency range have also been identified in  $\text{ZnWO}_4$  by Raman spectroscopy and associated with internal vibrations of the distorted  $\text{WO}_6$  octahedra<sup>22-24</sup> on the basis of frequencies quoted for a regular  $\text{WO}_6$  octahedron.<sup>25</sup> A full assignment of the powder infrared (IR) data presented here is not, however, possible: Further polarized single crystal studies are required for a more detailed analysis.

Group theoretical considerations show that  $3N = 36$  vibrational modes are expected in both the  $P2/c$  and  $P\bar{1}$  structures of  $\text{Zn}_{0.75}\text{Cu}_{0.25}\text{WO}_4$ . The total representation of the  $P2/c$  unit cell contains 18 Raman-active modes ( $8A_g + 10B_g$ ), 15 infrared-active modes ( $7A_u + 8B_u$ ), and 3 acoustic vibrational modes ( $A_u + 2B_u$ ). These are correlated to  $18A_g$  (Raman) +  $15A_u$  (IR) +  $3A_u$  (acoustic) modes in the low-symmetry  $P\bar{1}$  structure. Any soft mode would have the symmetry of the active representation for the transition  $B_g$ , and would be Raman active, but the hard modes observed in the midinfrared spectra recorded here couple bilinearly to the order parameter for the transition  $Q$ , as measured on a phonon time scale (and correlated over much shorter distance than the previous x-ray work<sup>10</sup>). Modes may be assigned, therefore, on the basis of their temperature dependence. The symmetry change at the high-temperature phase transition has, for example, a direct effect on temperature dependence of the mode at 1191  $\text{cm}^{-1}$ , which softens markedly on increasing temperature and moves close to the 1112- $\text{cm}^{-1}$  band at around 570 K (Fig. 2). Since the frequencies of internal modes of the  $\text{WO}_6$  octahedra are generally relatively independent of temperature,<sup>23</sup> it seems that the resonances observed at 1112 and 1191  $\text{cm}^{-1}$  are not associat-

ed with the  $\text{WO}_6$  octahedra, but with  $(\text{Zn,Cu})\text{O}_6$  internal vibrations, which are expected to play a more significant part in driving the transition.

The theory of coupling between hard modes and structural phase transitions was formulated by Petzelt and Dvorak.<sup>26</sup> The essential result for a nondegenerate hard mode in terms of the expected frequency changes is that in the lowest order

$$\Delta\omega^2(T) = (\langle\omega\rangle - \omega)(\langle\omega\rangle + \omega) = \delta Q^2(T),$$

and since  $(\langle\omega\rangle + \omega) \approx \text{constant}$  this also implies  $\Delta\omega(T) \propto Q^2(T)$ . This contrasts with the linear relationship between the frequency of a soft mode and the order parameter.

The temperature evolution of the frequency of the measured absorption bands is shown in Figs. 3 and 4. There is a significant change in  $\partial\omega/\partial T$  at  $570 \pm 5$  K for four bands: those near 1190, 1110, 670, and  $540 \text{ cm}^{-1}$ . This is the same temperature (within experimental error) as  $T_c$  measured by x-ray diffraction, and the observed changes in hard-mode phonons are inferred to result from the expected coupling to  $Q$ .

Frequency shifts are greatest for the  $1190\text{-cm}^{-1}$  phonon, which decreases in frequency steadily and slowly on increasing temperature, with a more rapid jump of more than  $20 \text{ cm}^{-1}$  at or near  $T_c$ . This behavior appears to indicate first-order behavior of a thermodynamic order parameter, if the frequency shifts are coupled in the expected manner. Frequency shifts are smaller for modes at 1110, 670, and  $540 \text{ cm}^{-1}$ , although the latter could be interpreted as showing  $\Delta\omega \propto Q^2 \propto (T_c - T)$  below  $T_c$ , in agreement with observations of the macroscopic order parameter from x-ray measurements.<sup>2</sup>

The varying temperature-dependent behavior of the hard modes measured here may be summarized as three types. First, there are those which are not influenced by the transition, secondly, those (at 670 and  $540 \text{ cm}^{-1}$ ), which show changes  $\Delta\omega \propto Q^2$  corresponding to those pre-

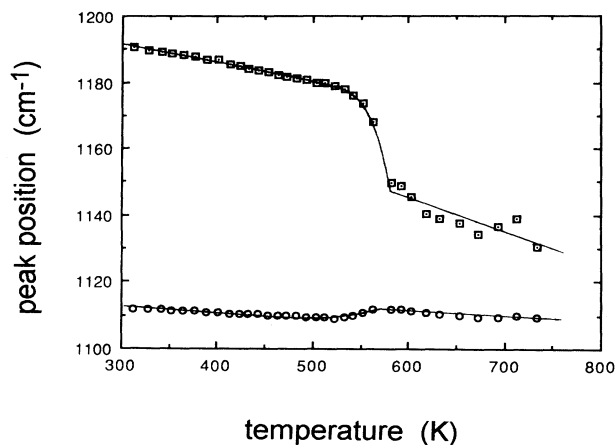


FIG. 3. Temperature dependence of the  $1190$  and  $1110\text{-cm}^{-1}$  absorption bands. The changes below  $570 \pm 5$  K result from coupling of these hard modes to the short-range order parameter for the transition. Solid lines are drawn through the data points as guides to the eye.

dicted from the thermodynamic theory for the macroscopic order parameter, and thirdly, those (at  $1190$  and  $1110 \text{ cm}^{-1}$ ), which show changes  $\Delta\omega \propto Q^2$  corresponding to a more first-order transition behavior and, which display a quasidegeneracy above  $T_c$ . In these respects the phonon behavior bears some resemblance to that ob-

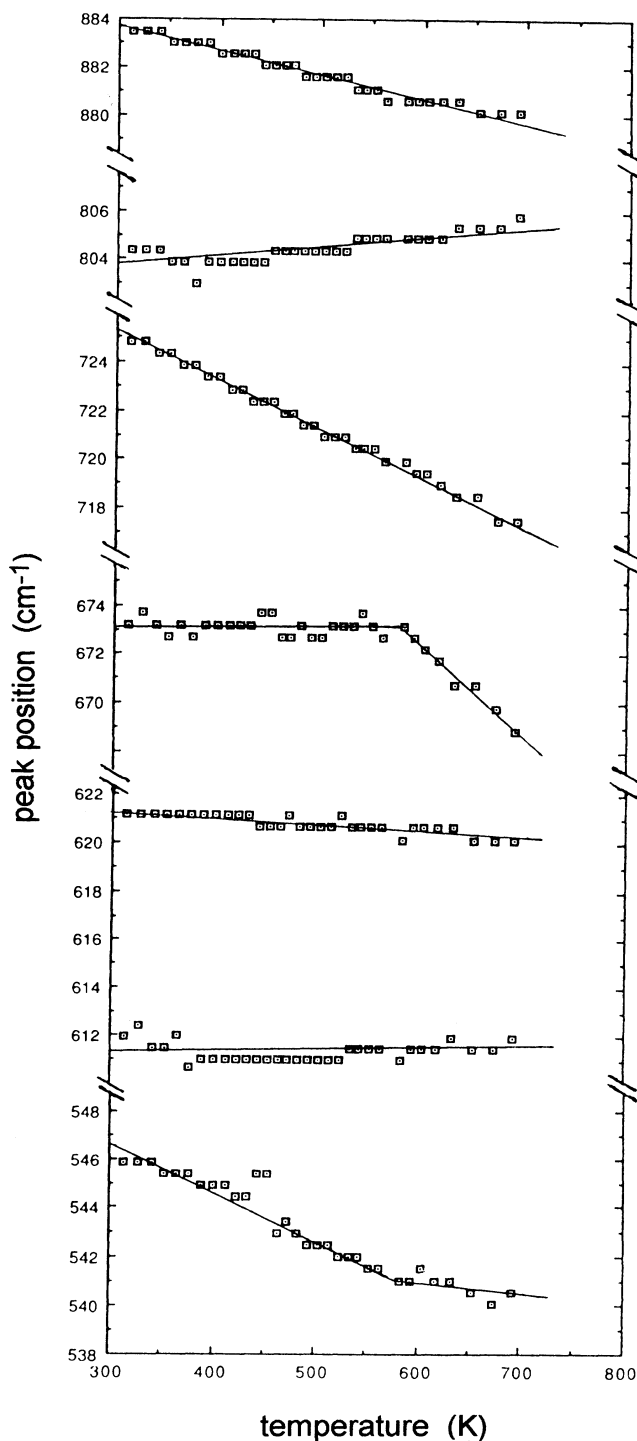


FIG. 4. Temperature dependence of absorption bands between  $1000$  and  $500 \text{ cm}^{-1}$ .

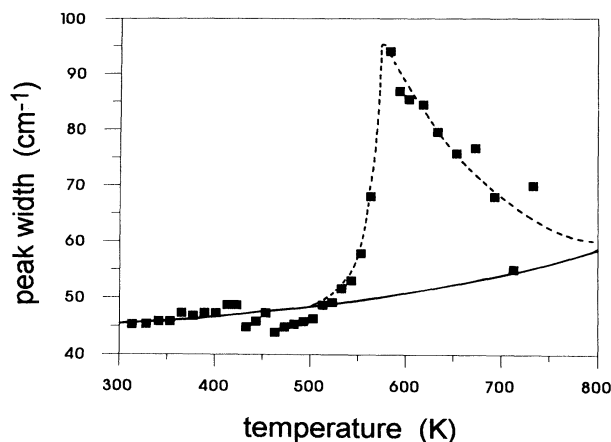


FIG. 5. Peak width full width at half maximum of the  $1190\text{-cm}^{-1}$  absorption band as a function of temperature. The solid and dashed lines serve as a guide to the eye and show the contributions from standard anharmonic interactions and dynamic transition-related fluctuations, respectively. The reduction of peak broadening above  $T_c$  suggests that the high-temperature phase is not a disordered average structure.

served at the order-disorder transition in triglycine sulfate.<sup>27</sup>

The characteristic length scale  $\xi$  of hard-mode phonons is related to their band width  $\Delta\omega$  and frequency  $\omega_0$  according to  $\xi \approx a / \pi(2\Delta\omega/\omega_0)^{1/2}$  where  $a$  is the lattice parameter,<sup>10</sup> so that this decreases with increasing frequency (and is typically less than  $10 \text{ \AA}$ ). This implies that the mode shifts at  $1190 \text{ cm}^{-1}$  may be due to more local effects than those at  $670$  and  $540 \text{ cm}^{-1}$ . Furthermore, in contrast to the other measured bands, the mode at  $1190 \text{ cm}^{-1}$  shows large variations in linewidth as a function of temperature (Fig. 5). This amounts to an increase of  $50 \text{ cm}^{-1}$  on the width of the  $1190\text{-cm}^{-1}$  absorption band at  $T_c$ , compared with its width at room temperature.

The expected temperature dependence of the phonon damping factor  $\Gamma$  follows from multiphonon interactions and may be expressed as  $\Gamma_{o(T)} = \Gamma_{(T=0 \text{ K})} + AT + BT^2$ , where the residual line width at  $0 \text{ K}$  reflects broadening due to density of states effects. It is clear from Fig. 5 that there is an excess broadening near  $T_c$  over and above that expected from simple anharmonicity. The high-temperature data indicate that this excess line broadening  $\Gamma^*$  persists in the high-temperature paraphrase but does reduce to some extent on increasing temperature.

Such critical line broadening may result from dispersion of the hard mode, from finite spatial extent ( $\xi$ ) of a local precursor order parameter occurring on a modified coherent time ( $\tau$ ), or alternatively from a critical anomaly in the hard-mode self energy. Since the mode shifts by some  $50 \text{ cm}^{-1}$  around  $T_c$ , this final case may be more

significant than has previously been considered in hard-mode studies of phase transitions in other materials. The line broadening could certainly be correlated with potential mobile domain boundaries and precursor order in the vicinity of  $T_c$  [as has been suggested for  $\text{Pb}_3(\text{PO}_4)_2$  (Ref. 28),  $\text{KMnF}_3$  (Ref. 29), and more recently  $\text{CaAl}_{12}\text{Si}_2\text{O}_8$  (Ref. 11)]. Spatial inhomogeneity of the order parameter would also contribute. The reduction of  $\Gamma^*$  above  $T_c$  does suggest, however, that the high-temperature phase is not an average of dynamic low-symmetry domains, although precursor order in the monoclinic phase certainly appears significant up to at least  $T_c + 100 \text{ K}$ .

#### IV. CONCLUSIONS

The hard-mode behavior in  $\text{Zn}_{0.75}\text{Cu}_{0.25}\text{WO}_4$  may be understood if the  $1190\text{-cm}^{-1}$  phonon results from Cu-O vibration in the distorted Cu octahedra. The Jahn-Teller distortion on the Cu octahedra has  $\bar{1}$  symmetry, but the monoclinic mean field in the high-temperature phase frustrates such distortions at the Cu site. On approaching  $T_c$  from above the structural instability is triggered by a strain mediated isospin behavior at the Cu site, which fluctuates with increasing amplitude near  $T_c$ . The broadening of this absorption band in the vicinity of  $T_c$  arises either from interaction with solitonic excitations or the local flip motion at the Cu site. The observed broadening of certain Bragg reflexions in x-ray-diffraction studies may also be attributed to these dynamic processes. The phonon frequency shift below  $T_c$  indicates the space averaged local order parameter at the Cu site. This does not scale identically to the macroscopic order parameter, but is presumably coupled to it via strain. Hard-mode shifts of lower-frequency phonons accord with typical second-order behavior, in agreement with the observed macroscopic order parameter. Furthermore, line broadening is not observed for these lower-frequency phonons. Most absorption features between  $1000$  and  $500 \text{ cm}^{-1}$  are largely independent of temperature. It appears, therefore, that the structure may be thought of in terms of two features, the Cu octahedra, which locally relax to triclinic symmetry, and the remainder of Zn and W octahedral framework, which couples to the macroscopic triclinic order parameter directly but which shows higher order (and apparently weaker) coupling to the Cu-site distortion.

#### ACKNOWLEDGMENTS

The author is grateful for the provision of the sample by Dr. P. F. Schofield and the use of the FTIR facility at Department of Earth Sciences, University of Cambridge. This work was supported by NERC Grant No. GR9/255.

<sup>1</sup>P. F. Schofield and S. A. T. Redfern, *J. Phys. Condens. Matter* **4**, 375 (1992).

<sup>2</sup>P. F. Schofield and S. A. T. Redfern, *J. Phys. Chem. Solids* **54**, 161 (1993).

<sup>3</sup>P. F. Schofield, C. M. B. Henderson, S. A. T. Redfern, and G. van der Laan (unpublished).

<sup>4</sup>P. F. Schofield, Ph.D. thesis, University of Manchester, 1992.

<sup>5</sup>O. S. Filipenko, E. A. Pobedimskaya, and N. V. Belov,

- Kristallografiya **13**, 163 (1968) [Sov. Phys. Crystallogr. **13**, 127 (1968)].
- <sup>6</sup>L. Kihlborg and E. Gebert, Acta Crystallogr. B **26**, 1020 (1970).
- <sup>7</sup>J. B. Forsyth, C. Wilkinson, and A. I. Zvyagin, J. Phys. Condens. Matter **3**, 8433 (1991).
- <sup>8</sup>J. Petzelt and V. Dvorák, in *Vibrational Spectroscopy of Phase Transitions*, edited by Z. Iqbal and F. J. Owens (Academic, Orlando, 1984), pp. 55–151.
- <sup>9</sup>B. Güttler, in *Phase Transitions in Ferroelastic and Coelastic Crystals*, edited by E. Salje (Cambridge University Press, Cambridge, England, 1990), pp. 230–252.
- <sup>10</sup>E. K. H. Salje, Phase Trans. **37**, 83 (1992).
- <sup>11</sup>S. A. T. Redfern and E. Salje, Phys. Chem. Minerals **18**, 526 (1992).
- <sup>12</sup>E. K. H. Salje, A. Ridgwell, B. Güttler, B. Wruck, M. T. Dove, and G. Dolino, J. Phys. Condens. Matter **4**, 571 (1992).
- <sup>13</sup>A. Watterich, G. J. Edwards, O. R. Gilliam, L. A. Kappers, R. Capelletti, and B. Zelei, Phys. Lett. A **160**, 477 (1991).
- <sup>14</sup>A. Watterich, M. Wöhlecke, H. Müller, K. Raksányi, A. Breitung, and B. Zelei, J. Phys. Chem. Solids **53**, 889 (1992).
- <sup>15</sup>I. Földvári, R. Capelletti, L. A. Kappers, O. R. Gilliam, and A. Watterich, Phys. Lett. A **135**, 363 (1989).
- <sup>16</sup>I. Földvári, R. Capelletti, A. Péter, I. Cravero, and A. Watterich, Solid State Commun. **59**, 855 (1986).
- <sup>17</sup>H. Wang and S. Zhao, J. Solid State Chem. **73**, 356 (1988).
- <sup>18</sup>P. J. Born, D. S. Robertson, P. W. Smith, G. Hames, J. Reed, and J. Telfor, J. Lumin. **24/25**, 131 (1981).
- <sup>19</sup>S. K. Arora, T. Mathew, and N. M. Batra, J. Cryst. Growth **88**, 379 (1988).
- <sup>20</sup>S. K. Arora, T. Mathew, and N. M. Batra, J. Phys. Chem. Solids **50**, 665 (1989).
- <sup>21</sup>G. M. Clark and W. P. Doyle, Spectrochim. Acta. **22**, 1441 (1966).
- <sup>22</sup>Y. Liu, H. Wang, G. Chen, Y. D. Zhou, B. Y. Gu, and B. Q. Hu, J. Appl. Phys. **64**, 4651 (1988).
- <sup>23</sup>H. Wang, F. D. Medina, Y. D. Zhou, and Q. N. Zhang, Phys. Rev. B **45**, 10356 (1992).
- <sup>24</sup>J. F. Scott, J. Chem. Phys. **49**, 98 (1968).
- <sup>25</sup>P. Ahmad, L. Dixit, and N. K. Sanyal, Indian J. Pure Appl. Phys. **12**, 489 (1974).
- <sup>26</sup>J. Petzelt and V. Dvorak, J. Phys. C **9**, 1571 (1976).
- <sup>27</sup>V. Winterfeldt, G. Schaack, and A. Klöpperpieper, Ferroelectrics **15**, 21 (1977).
- <sup>28</sup>E. Salje, V. Devarajan, U. Bismayer, and D. M. C. Guimaraes, J. Phys. C **16**, 5233 (1983).
- <sup>29</sup>A. D. Bruce, W. Taylor, and A. F. Murray, J. Phys. C **13**, 483 (1980).